Co-funded by the European Union

Research Fund for Coal & Steel

Hybrid energy storage system using post-mining infrastructure (HESS)

Deliverable 4.3

Lining materials selection and properties

30.09.2025

PROJECT	
Project number	**101112380**
Project name	**Hybrid energy storage system using post-mining infrastructure**
Project acronym:	**HESS**
Call	**RFCS-2022**
Topic	**RFCS-01-2022-RPJ**
Type of action	**RFCS-PJG**
Service	**REA/B/01**

DOCUMENT PROPERTIES

Document Number	**D.4.3**
Document Title	**Lining materials selection and properties**
Document responsible	**SUT**
Target dissemination level	**PU - Public**
Document authors	**Konrad Kołodziej (SUT)** **Marcin Lutyński (SUT)**
Data of the document	**30.09.2025**

Table of contents

1. Introduction

1.1. Purpose and scope of Deliverable 4.3

This deliverable reports the measured gas-permeabilities of candidate shaft-lining materials and coating systems, together with the test methodology and tabulated datasets needed for engineering use in HESS. As a DATA deliverable, its core purpose is to provide traceable, quality-assured permeability values for representative "concrete + coating" configurations that could be applied to post-mining shafts intended for compressed-air operation. By replacing assumptions with measurements—clearly specifying pressure ranges, gas type, units and results variability, the document supplies the evidence base required to judge whether lining systems can achieve the tightness needed under cyclic loading.

The gas-tightness of the shaft lining is critical. Even without visible cracking, concrete's connected pore network can permit pressure-driven gas transport, causing standby losses over long idle periods. During extended idle periods, such a phenomenon leads to the gradual loss of compressed air and a reduction in the overall efficiency of the storage system. For this reason, it is necessary to apply protective coatings providing high resistance to gas permeation, and their selection requires laboratory verification of effectiveness—particularly through gas permeability measurements of the "concrete + coating" system within the pressure ranges characteristic of ACAES(adiabatic compressed air energy system) operation.

The scope is intentionally narrow and practical. We describe how specimens were prepared and conditioned, how gas flow was measured and reduced to intrinsic permeability, and how repeatability was managed. Results are presented in readable tables to facilitate direct reuse in design checks and modelling. Where helpful, we illustrate the translation from material-scale permeability to indicative leakage at component scale; however, such illustrations are provided only as a reading guide and do not substitute for detailed reservoir or system models developed elsewhere in the project.

Equally important is what this document does not cover. Ageing and chemical durability, thermal cycling effects linked to TES coupling, mixed-gas behaviour, and application/constructability topics are outside the remit of D4.3 and are addressed in other HESS outputs. Here we focus on the single property—gas permeability—that acts as the primary gating criterion for using existing shafts as pressure vessels within the hybrid storage concept.

The data will be used immediately downstream to shortlist lining/coating systems that meet target permeability under relevant pressures; provide calibrated leakage inputs to mechanical and thermal integration activities; and inform techno-economic and environmental assessments through quantified standby losses and sensitivity bounds. In short, D4.3 converts laboratory measurements into dependable inputs for design decisions across the project, ensuring subsequent work builds on validated lining performance rather than on baseline assumptions.

The following subchapter situates this measurement programme within the broader HESS concept and explains the project context and role of WP4.

1.2. Project context and role of WP4

Deliverable D4.3 – *Selection and properties of lining materials* constitute a dedicated component of Work Package 4, focused on the issue of concrete lining permeability and the effectiveness of protective coatings applied inside the shaft. The document is of a pre-operational nature and serves three essential functions: it organizes and standardizes the methodology for assessing gas permeability, it presents experimental data in the form of tabulated datasets, and it provides the basis for engineering interpretation required for material selection and for the choice of protective systems in subsequent WP4 tasks. Particular emphasis is placed on identifying and preliminarily selecting sealing coatings capable of reducing gas migration through the porous structure of the shaft's concrete lining.

The analysis is embedded within the framework of normative requirements: the classification of surface protection systems according to EN 1504-2, which distinguishes hydrophobic impregnation, impregnation, and film-forming coatings [1]. In the perspective of mine shaft adaptation, protective coatings that create a continuous barrier reducing gas permeability are of key importance. Application and control requirements are defined in EN 1504-10, which cover, among others, the preparation of the concrete substrate, moisture control prior to application, assurance of coating continuity and thickness, as well as acceptance procedures [2]. These aspects are reflected in the methodological section of the present report.

1.3. Research problem: gas transport in shaft casing

In the adaptation of mine shafts into compressed gas storage facilities, a key issue is the limitation of gas migration through the concrete lining. Concrete, due to its porous and heterogeneous structure, exhibits a complex transport mechanism. Permeability is influenced by gel and capillary pores within the cement paste, the interfacial transition zone (ITZ) around the aggregate, as well as microcracks developing under the influence of shrinkage, thermal cycles, and mechanical loading [3].

In this Deliverable, the research problem is formulated as the following question: to what extent can coatings, such as epoxy and polyurea systems, effectively reduce the intrinsic permeability coefficient k of the "coating–concrete" system (for concretes C20/25 and C40/45) under working pressures corresponding to ACAES operation.

By adopting the research hypothesis: "a properly applied continuous coating reduces the value of k by at least one order of magnitude compared to uncoated concrete." Engineering experience from tunnels and reservoirs indicates that the cementitious matrix alone rarely ensures long-term tightness, and the use of coating systems appears to be the only viable solution for existing structures.

1.4. Objectives and scope of Deliverable D4.3

The objective of Deliverable D4.3 is to determine the effectiveness of protective coatings in reducing gas permeability through the concrete lining of mine shafts and to develop a methodology for assessing this phenomenon under laboratory conditions. The document provides results essential for evaluating the feasibility of practical shaft adaptation for Compressed Air Energy Storage (ACAES) and serves as a basis for further material analyses carried out within WP4.

The scope of work includes:

- the selection and characterization of two coating systems compliant with EN 1504-2 [1], representing different approaches to concrete protection (a thin-layer epoxy coating and a thicker-applied Xolutec® membrane),

- the use of C20/25 and C40/45 concrete substrates prepared in accordance with EN 206 and EN 12390-2 [4–5], where the lower-class concrete serves as the base for coating application, while the higher-class concrete acts as the reference,

- the performance of air permeability measurements using the steady-state flow method within pressure ranges characteristic of ACAES operation, employing helium as test gas and accounting for the Klinkenberg correction [6–8],

- the development of an engineering interpretation of the results, including the translation of laboratory values into potential compressed air losses at the shaft scale,

- embedding the results within the framework of normative requirements defined in EN 1504-2 and EN 1504-10 [5,9].

1.5. Restoration of aged shaft linings and rationale for sealing

Mine shafts that have been in operation for 30 to 50 years typically show distinct signs of concrete lining degradation. Although the structural load-bearing capacity is often retained, long-term exposure to groundwater, cyclic stresses, and chemical influences gradually weakens the lining. Common deterioration mechanisms include carbonation of the surface zone, leaching of calcium hydroxide, microcracking from shrinkage and thermal cycles (figure 1), and local spalling or delamination under variable hydrogeological conditions [10–16]. In shafts affected by aggressive mine waters, deposits, corrosion staining, and scaling are frequently observed, all of which reduce the continuity and integrity of the lining.

Figure 1 Degraded shaft lining after several decades of operation[17]

Such degradation directly affects the feasibility of using shafts as compressed-gas reservoirs. Even in the absence of visible large-scale damage, the interconnected pore structure of aged concrete permits pressure-driven gas migration, leading to standby losses that reduce storage efficiency. For this reason, restoration of the lining surface is an essential step before applying any protective sealing system.

The process begins with inspection and mapping of defects, followed by removal of loose or weakened material. Cracks and cavities are repaired with cementitious mortars compliant with EN 1504-3 to restore structural continuity. Once the geometry is re-established, surface preparation is carried out in accordance with EN 1504-10: laitance and contaminants are removed, pores are opened, and substrate moisture is controlled to provide reliable adhesion conditions.

The strength of this approach lies in its twofold effect: preserving the structural role of the lining while enabling the installation of surface protection systems that can reduce gas permeability by several orders of magnitude. Its main limitation is the dependence on execution quality—improper preparation or uncontrolled substrate conditions can compromise adhesion and coating continuity. Nevertheless, combining restoration with modern surface sealing represents the only practical pathway to convert legacy shafts into pressure-retaining reservoirs for energy storage, bridging the gap between existing mining infrastructure and present-day operational requirements [5,9,10–11].

1.6. Innovation and research gap

To date, the assessment of the durability of cementitious structures has been dominated by parameters related to water transport (water absorption, water permeability), whereas in ACAES applications the working medium is air. This elevates gas permeability to the role of a primary parameter, directly determining the ability to maintain pressure over extended periods and defining the balance of losses during standby cycles.

A critical gap remains: the lack of consistent data for concretes typical of shaft linings, featuring realistic porosity and a controlled, reproducible level of moisture, together with their comparison to coatings applied under conditions approximating that underground, and the subsequent calibration of laboratory values against real-world data. Existing reports highlighting the strong barrier effect of epoxy against air transport in other applications (e.g., tubular structures), as well as the high effectiveness and durability of polyurea in tunnel infrastructure with respect to liquid seepage, provide important context but do not replace dedicated gas validation in the "coating–shaft concrete" configuration [2,3].

The innovative aspect of D4.3 lies in shifting the emphasis from general durability indicators to a direct, metrologically rigorous assessment of gas transport in systems representative of shaft conditions, and in their interpretation at the ACAES system scale. Combining two distinct barrier philosophies (epoxy vs. polyurea) with flow measurement makes it possible not only to compare the coatings themselves but, above all, to estimate the impact of material choice on actual compressed air losses in the facility. In effect, D4.3 provides the missing link between the technical concept of the installation (including the patented ACAES shaft solution) and the practical selection and evaluation of protective coatings compliant with EN 1504-2/-10 - explicitly addressing the gap at the interface between materials engineering and the operation of underground energy storage [2,3,17–18]. Furthermore, it is intended to confirm both the validity and necessity of coating application, while providing the basis for quantifying the difference in operational losses in the absence of coatings, thereby enabling the assessment of the economic value of such an approach.

2. Materials

2.1. Concrete substrates of shaft casings and ACAES requirements

The practice of mine shaft construction has evolved alongside technological development and the increase in mining depths. In historical projects, particularly before the unification of standardization, concretes with parameters corresponding to classes lower than today's C20/25 were commonly used, resulting from limited quality control of cement, aggregates, and curing conditions [10–11]. These materials provided sufficient load-bearing capacity in shallower shafts, where rock mass pressure and hydrogeological influences were relatively minor [10].

With increasing shaft depths and the growth of mechanical and hydrogeological loads, higher-class concretes (corresponding to today's C25/30–C30/37) began to be widely applied from the 1960s onwards, while in the 1980s and 1990s, deep shafts routinely employed classes B40–B50 (≈ C32/40–C40/50). This practice was driven by the need to ensure greater strength, reduced water permeability, and long-term durability of the lining [9–11]. Mining guidelines specified in standards PN-G-05015 and PN-G-05016 defined the principles for shaft lining design and expected loads, supporting the use of higher-class concretes in shaft sections particularly exposed to rock mass pressure or water [9–10].

In the present study, two concretes were selected to reflect these conditions. C20/25 represents older shafts or those with lower requirements in terms of strength and watertightness, serving

as a more porous substrate with higher baseline permeability. C40/45, by contrast, serves as the uncoated reference, corresponding to modern deep shaft designs, where reduced water permeability and lining durability are key requirements [9–11].

From the perspective of ACAES, the geometric scale is critical: the economic viability of compressed air storage systems arises only at certain capacities and power levels, which directs attention to deeper shafts and/or those with larger diameters [1,2]. In such structures, the material requirements for the shaft lining naturally increase, particularly with respect to strength, water resistance, and—under energy applications—low gas permeability. The selection of the C20/25–C40/45 pair therefore allows the separation of the effect of concrete class from that of protective coating on gas transport, and the reproduction of scenarios ranging from older structures to target deep shafts that may be adapted for ACAES storage [1–2, 10–11].

Concrete mix preparation and specimen fabrication were carried out in accordance with EN 206 (concrete specification and conformity) and EN 12390-2 (making and curing specimens) [4–5]. The specimen geometry was standardized to cylinders Ø 25 mm × 30 mm. Although this differs from the RILEM standard (disc 150 × 50 mm), the literature provides precedents for the use of smaller cylinders in gas permeability testing, which justifies this approach provided that data are correctly reduced to account for the actual cross-sectional area and flow path length [22,12–13]. In order to reflect the main approaches to sealing concrete shaft linings, two contrasting types of surface protection were selected for testing: a dense thin-film barrier, representing solutions focused on minimising gas permeability on sound substrates, and a thicker coating capable of bridging cracks and accommodating substrate movements. Together they cover the typical range of conditions expected in aged and deep mine shafts, allowing the study to demonstrate both the potential and the limitations of coating-based reduction of gas transport under ACAES operating pressures.

Having defined the concrete substrate and ACAES-driven performance requirements, we now turn to the surface protection systems that provide the required gas-tightness. Section 2.2 summarises candidate coatings and membranes selected for laboratory verification, focusing on properties that govern permeation and durability on shaft linings: coati, crack-bridging class, water-vapour diffusion (H_2O), CO_2 diffusion, chemical and hydrostatic resistance, and pull-off adhesion to prepared concrete. For each system, we list its intended EN 1504-2 function(s), substrate preparation requirements, curing conditions, and practical constraints relevant to application in deep shafts. These characteristics frame the permeability tests that follow and justify the shortlist carried forward to the Results and Discussion.

2.2. ® WallCoat T - Epoxy Thin layer

WallCoat T is a representative example of a two-component, water-dispersed epoxy resin designed for the protection of concrete surfaces. From a chemical perspective, once the components are mixed and cured, this coating forms a three-dimensional polymer network which dense structure limits the penetration of gases and liquids. These properties are the result of the cross-linking process between the epoxy resin and the amine hardener, which leads to the formation of a film with high cross-sectional density and low porosity. In the context of adapting mine shafts for Compressed Air Energy Storage (ACAES), such a coating serves as a

barrier that potentially reduces the permeability of the concrete lining to air and technical gases, limiting losses during standby cycles. Properties of WallCoal T are presented in Table 1. From a normative perspective, WallCoat T belongs to surface protection systems according to EN 1504-2, where it is classified as a film-forming coating. It performs three basic functions: protection against fluids ingress, moisture regulation, and increasing surface resistivity [1]. These functions correspond to the operational requirements of structures exposed to the action of gaseous and liquid media. Detailed technical properties and material requirements, such as dry film thickness, capillary absorption, water vapor permeability, abrasion resistance, CO_2 barrier capacity, and mixture density, are summarized in Table 1.

Table 1 WallCoat T

Technical Parameter	**Value / Class**	**Notes on normative conformity**
Product Type	Two-component epoxy resin, waterborne	—
Classification of the protection system	Concrete Surface Protection System (CE)	EN 1504-2
Features by EN 1504-2	Ingress protection (1.3), humidity control (2.2), resistance enhancement (8.2)	EN 1504-2
Dry Coating Thickness (DFT)	~0,25 mm (typical)	—
Unit consumption	~0,28 kg/m² per layer	—
Density of the mixture	~1,39 kg/dm³	—
Solid Parts Content	~50% obj., ~64% by weight	—
Capillary Absorbency	w < 0,1 kg/(m²·h^0,5)	Compatibility with EN 1062-3
Vapour permeability	Class I, sD < 5 m	Compatibility with EN ISO 7783
CO_2 barrier	sD > 50 m	Compatibility z EN 1504-2 / DoP
Abrasion resistance (Taber)	~94 mg (CS10/1000 g/1000 Cycles)	—
Substrate temperature range	+10…+35 °C	—
Ambient temperature range	+10…+40 °C	—
Max. relative humidity	≤ 75%	—
Dew point requirement	+3 °C	—

Technical Parameter	Value / Class	Notes on normative conformity
Protection against moisture application	after min. 24 h	—

The epoxy coating limits both the diffusion of gas molecules under steady-state conditions and the flow induced by a pressure gradient. Its effectiveness depends on parameters such as: Water vapor permeability – determined according to EN ISO 7783, classified as Class I (sD < 5 m, equivalent air layer thickness below 5 meters, determined according to EN ISO 7783 by the water vapor permeability test of coatings). In practice, this means that the coating does not constitute a total barrier but restricts water vapor transport in a controlled manner, protecting the concrete from moisture ingress and the formation of microcracks [14]. Capillary absorption tested according to EN 1062-3, characterized by values below 0.1 kg/(m²·h^0.5). This parameter demonstrates effective protection against water ingress into the porous structure of concrete, which is important for reducing dissolved gas migration [15]. CO_2 barrier capacity – expressed by an equivalent air layer thickness sD > 50 m (equivalent air layer thickness above 50 meters, determined according to EN 1062-6 by the coating permeability test for CO_2) in accordance with EN 1062-6. The high value indicates strong resistance of the coating to concrete carbonation and, at the same time, effectiveness in limiting gas diffusion [16].

Abrasion resistance – tested by the Taber method, confirming the suitability of the coating in conditions where local mechanical loads may occur during operational work [23]. Adhesion to the substrate – verified according to EN 1542 by the pull-off method, which is a key condition for maintaining barrier continuity. Tests show that well-prepared epoxy coatings achieve adhesion exceeding the minimum requirements of the standard [24].

Numerous studies confirm the effectiveness of epoxy coatings in reducing gas transport through concrete. Kim et al. [25] demonstrated that the application of a thin epoxy layer on ordinary concrete significantly reduces the air permeability coefficient, which is directly relevant to structures exposed to internal pressure. Park [26] demonstrated the effectiveness of epoxies as an anti-carbonation barrier, which is particularly important in the context of long-term protection. Cabrera et al. [27] indicated the role of coatings in reducing CO_2 permeability, while Li et al. [28] described comparative adhesive properties and gas penetration resistance of epoxy and polyurethane systems. Liu et al. [28] confirmed the barrier stability of epoxy coatings in air and technical gas permeability tests, indicating their suitability under underground conditions.

Summary. WallCoat T, as a thin-layer epoxy coating, combines features beneficial from both chemical and engineering perspectives: a dense polymer structure, high resistance to gas diffusion, and compliance with normative requirements. Its effectiveness depends equally on material properties and application quality. The parameters summarized in Table 1, together with literature data, confirm the validity of its use as a protective barrier in shaft linings prepared for ACAES operation.

2.3. Sikagard® M 790 — membrane Xolutec®

Sikagard® M 790 is a two-component, thermosetting protective membrane developed with Xolutec® technology. This technology is based on the concept of a cross-linked polymer network (XPN), where polymer segments form a mutually interpenetrating structure. This makes it possible to control the cross-link density and morphology of the coating, resulting in high chemical and mechanical resistance as well as long-term operational durability. Xolutec® is the trade name of a system developed by Sika, in which the polymer architecture has been optimized for barrier performance and the ability to accommodate local substrate deformations.

Once cured, the material forms a dense, homogeneous structure with a high cross-link density. Such a structure limits the penetration of gas and water molecules, reduces capillary ingress into the coating, and improves resistance to stress concentration in areas of substrate defects. The thick-layer character of the membrane summarized in Table 2, provides an additional material margin, which reduces the impact of local damage and supports barrier continuity.

Table 2. Sikagard® M 790

Technical Parameter	Value / Class	Standard/Test Method
Product Type	Two-component, thermosetting Xolutec membrane®	—
Classification of the protection system	Concrete Surface Protection System (CE)	EN 1504-2
Features by EN 1504-2	Ingress protection, humidity regulation, increased surface resistance	EN 1504-2
Dry Coating Thickness (DFT)	0.7 - 0.8 mm (typical); up to 1.1 mm in a chemical environment	—
Unit consumption	~0,8–1,2 kg/m² (depending on the application)	—
Capillary Absorbency	0,0005 kg/(m²·h^0,5)	EN 1062-3
Vapour permeability	Class III, sD = 126 m	EN ISO 7783
Barrier CO_2	sD = 206 m	EN 1062-6
Water resistant	5 bars (positive); 2,5 bar (Negative pressure)	—
Crack bridging	Class A3 (Static, >0,5 mm @ 23 °C); Class B3.1 (Dynamic)	EN 1062-7
Adhesion to concrete (pull-off)	~2,9 MPa (dry); ~2,2 MPa (Wet)	EN 1542
Abrasion resistance (Taber)	~194 mg	ASTM D4060
Hardness	Shore D ~80	—
Tensile strength	>20 MPa	—
Impact resistance	24,5 Nm (class III)	—

Substrate/ambient temperature range	+5…+35 °C	—
Substrate moisture	No restriction (no condensation)	—
Pressurized water resistance time	~24 h	—
Full curing	7 Days @ 20 °C	—
Recommended Ground	Sikagard® P 770	—

From the perspective of normative classification, the membrane belongs to surface protection systems for concrete according to EN 1504-2 (film-forming coating), fulfilling the functions of protection against ingress, moisture regulation, and increasing surface resistivity [1]. For applications in shaft linings operating under ACAES conditions, two groups of properties are particularly relevant: the barrier transport parameters of the film (water vapor permeability and CO_2 resistance, expressed as equivalent air layer thickness — sD for water vapor according to EN ISO 7783 and sD, CO_2 for carbon dioxide according to EN 1062-6) and crack-bridging ability assessed by the method specified in EN 1062-7 [29,30,31,32]. Numerical values are not repeated in the text — they are summarized in Table 2.

Barrier parameters reflect the film's ability to limit the transport of water vapor and gases. High sD, CO_2 values (equivalent air layer thickness in meters, determined according to EN 1062-6) indicate high resistance to carbon dioxide diffusion and thus effective protection against concrete carbonation. Water vapor permeability, classified according to EN ISO 7783 (sD — equivalent air layer thickness for water vapor), indicates controlled vapor transport, which prevents excessive moisture accumulation while maintaining the protective function [29,31]. A very low capillary water absorption, measured in accordance with EN 1062-3, limits water ingress into the near-surface zone and reduces the risk of phenomena facilitating gas migration, for example through the dissolution and transport of gaseous components in the liquid phase [30].

In the specialist literature, crack-bridging membranes are evaluated using procedures compliant with EN 1062-7. Experimental studies indicate that the crack-bridging class depends on the dry film thickness, test temperature, and the type of loading (static/dynamic). Schiessl and Breit demonstrated in dynamic tests that resistance to cyclic crack opening increases with film thickness and the stability of adhesion at the coating–concrete interface [33]. Xu, Zhang, and Li presented an evaluation of protective crack-bridging coatings on concrete structures, showing the relationship between the mechanical parameters of films and the achieved crack-bridging classes [34]. Research by Gonzalez et al. [35] demonstrates that the long-term durability of such systems in aggressive environments depends on polymer cross-linking quality and adhesion stability.

Application aspects and quality control should be carried out in accordance with EN 1504-10 [9]. These include substrate preparation (cleaning, removal of cement laitance, mechanical pore opening), control of substrate moisture and temperature, as well as ambient conditions (maintaining a margin above the dew point), and ensuring uniform dry film thickness. For quality reasons, it is recommended to verify film continuity, i.e., eliminating through-pores and

surface pinholes, which represent pathways for gas migration. Adhesion testing by the pull-off method according to EN 1542 [35] allows the effectiveness of the application to be assessed. The technical datasheet provides for the possibility of application on substrates with elevated moisture (without condensation) and the use of a suitable primer to improve wetting and reduce the risk of surface defects — detailed technological recommendations are included in the manufacturer's documentation [36].

2.4. Rationale for selection and comparative configuration

The selection of protective coatings for use in the linings of shafts adapted as compressed air storage facilities requires accounting for a set of criteria arising both from normative requirements and from the operational conditions of ACAES systems. Of particular importance are barrier performance against gases and water vapor, crack-bridging capacity, mechanical resistance, and technological aspects related to coating application and quality control. According to EN 1504-2:2004 *Products and systems for the protection and repair of concrete structures – Part 2: Surface protection systems for concrete,* both coatings analyzed - WallCoat T (Table 1) and Sikagard® M 790 (Table 2) - are classified as surface protection systems for concrete, fulfilling the functions of protection against ingress, moisture regulation, and increasing surface resistivity. They differ, however, in their chemical design philosophy and range of functional properties, which justifies their separate discussion and comparison.

WallCoat T, as a thin-film epoxy coating, represents a solution with a relatively low dry film thickness (DFT), typically ~0.25 mm. Its barrier effectiveness relies on low capillary absorption and high resistance to CO_2 diffusion, which limits concrete carbonation and gas migration through the substrate. The high cross-link density of epoxy systems promotes the formation of coatings with very low permeability, but at the same time reduces their ability to accommodate deformations and restricts crack-bridging capacity. The literature emphasizes that epoxies demonstrate excellent barrier performance but may be sensitive to application conditions, particularly substrate moisture, which negatively affects adhesion and film continuity [25–27]. In the context of ACAES, this implies that WallCoat T is most suitable for shafts with well-prepared and stable linings, where the risk of cracking and deformation is limited.

Sikagard® M 790, based on Xolutec® technology, provides a thick-film alternative in which barrier performance is complemented by crack-bridging capacity. Xolutec® technology is based on the concept of a cross-linked polymer network (XPN), allowing control of cross-link density and tailoring of chemical and mechanical properties. This results in a dense, highly cross-linked structure offering strong chemical resistance and the ability to accommodate local substrate deformations. Typical dry film thickness values, ranging from 0.7–1.1 mm, are several times greater than those of epoxy coatings, providing an additional margin of material that enhances barrier continuity even under dynamic loading. Studies by Schiessl and Breit [33] show that crack-bridging stability under cyclic loading depends on film thickness and adhesion quality, which is consistent with observations for Xolutec® systems. In practice, this means that the M 790 membrane can be used in shafts exposed to cracking, periodic moisture, and variable mechanical loads. An additional advantage is the possibility of application across a broader range of climatic conditions, including on substrates with elevated moisture, while still complying with EN 1504-10:2017 [9].

When comparing the two systems, it should be highlighted that WallCoat T is characterized by lower material consumption and simpler thin-film application, but requires precise control of environmental conditions (moisture, substrate temperature). Sikagard® M 790, although associated with higher material consumption and the need for specialized two-component spraying equipment, offers a broader application window - including suitability for moist substrates - as well as higher mechanical and dynamic resistance. Operationally, this implies that the epoxy coating WallCoat T is more appropriate for structures with low deformation and stable geomechanical conditions, whereas the Xolutec® M 790 membrane is preferred in deeper shafts with a higher risk of cracking, where greater coating flexibility and durability are required.

Economic considerations must also be taken into account. WallCoat T, with its lower material consumption and thinner film thickness, may be a more cost-effective solution in applications with moderate requirements [37]. By contrast, M 790, despite higher material and technological demands, provides greater operational security under higher-risk conditions, which in the long term may offset its higher investment costs [38]. Comparative studies suggest that crack-bridging systems, even at a higher unit price, yield benefits in the form of reduced repair costs and lower operational losses [39].

In summary, both coatings meet the normative requirements of EN 1504-2 and can be used in ACAES systems, but their properties make them suited to different scenarios. WallCoat T should be regarded as a reference solution for structures with high-quality concrete and limited risk of cracking, whereas Sikagard® M 790 is dedicated to more demanding environments that require crack-bridging capacity and moisture resistance. Identifying differentiating parameters—such as equivalent air layer thickness sD (m), capillary absorption, and crack-bridging class enables an engineering assessment of the suitability of both systems. From both a design and operational perspective, the two technologies should be regarded as complementary elements within a suite of protective materials tailored to the specific shaft and its operating conditions.

3. Methodology of Steady-State Flow Air Permeability Testing

3.1. Significance of steady state

A steady state is understood as a temporal plateau of $_{pu,pd}$, T, and q with no systematic drift. This condition is necessary to interpret the flow within the Darcy framework and to distinguish true transport through the specimen from transient storage in dead volumes and from regulator dynamics. As shown by Heap and Kennedy [40], in materials with extremely low permeability (small k) the approach to steady state can be prolonged, because the system time constant increases with the specimen's hydraulic resistance and with the combined compressible "capacity" of the gas–apparatus ensemble. In this regime even fluctuations on the order of a few pascals are significant: they modulate $\Delta(p^2) = p^2_u - p^2_d$ and thereby directly bias the estimate of k (since $k \propto q p \alpha / \Delta(p^2)$).

The choice of measurement medium governs both the time required to reach steady state and the detection resolution [40]. Lower-viscosity gases (e.g., H_2) shorten hydraulic transients and increase the measured *q*, but at low *p* they more strongly reveal slip (Klinkenberg) effects, making the result more "apparent." Conversely, higher-viscosity media (e.g., He relative to H_2) better damp short-period pressure oscillations, at the cost of smaller flows and a higher detection limit.

3.2. General assumptions

Gas permeability *k* is evaluated in the Darcy regime using a compressible-flow formulation that preserves linear proportionality between the measured flow and the driving force. For a specimen of length *L* and cross-sectional area *A*, traversed by a single-phase gas of dynamic viscosity μ at temperature *T*, the steady volumetric flow rate *q* relates to *k* through the squared-pressure form of Darcy's law [41]:

$$k = \frac{2qp_d dL\mu}{A(p_u^2 - p_d^2)}$$

where p_u and p_d denote the absolute inlet and outlet pressures, respectively, and $\Delta = (p^2) = p^2_u - p^2_d$ accounts for gas compressibility while retaining linearity in the Darcy limit. The mean pressure in the specimen is $\bar{p} \approx (p_u + p_d)/2$ and is reported alongside *k* to indicate the thermodynamic state of the measurement.

3.3. Rationale for choosing helium as the sole measurement medium

In this study, helium is used exclusively as the measurement gas. As described by Villar et al., helium, due to its small kinetic diameter (~0.26 nm), reveals the finest transport pathways. [22] further emphasized its lack of adsorption on pore walls, which means that the signal corresponds to pure mass flow. Heap and Kennedy [40] demonstrated that helium, owing to its low viscosity, allows for faster attainment of steady state and enables the detection of extremely small q values. Moreover, the comparability of results at the laboratory scale justifies its widespread use - already indicated in the earlier work of Brace et al. [42]. Finally, helium is chemically inert and non-toxic, which increases the safety of experimental procedures.

For comparison: the kinetic diameter of oxygen (O_2) is ~0.346 nm, and that of nitrogen (N_2) is ~0.364 nm. The larger molecular sizes of these gases make them less sensitive for detecting flows through micropores, while at the same time more prone to adsorption interactions. This further justifies the selection of helium as the test gas offering the highest metrological resolution.

3.4. The Klinkenberg effect and the extrapolation procedure

Gas slippage at pore walls, first identified by Klinkenberg [43], makes the **apparent** permeability increase as the mean pressure decreases. In the low-Knudsen regime relevant here, the effect is well represented by the linear Klinkenberg relation [42,44]

$$k_{app}(\bar{p}) = k_{\infty}(1 + \frac{b}{\bar{p}})$$

where $\bar{p}=(p_u + p_d)/2$ is the mean absolute pressure in the specimen, k_∞ is the intrinsic (slip-free) permeability, and *b* is the gas- and material-dependent slip factor. This form reflects the first-order relaxation of the no-slip boundary condition at rarefied pore-scale flow and has been routinely used in subsequent studies, including Heap and Kennedy [40].

To obtain k_∞ *b* experimentally, measurements are performed at multiple steady-state plateaus spanning a range of $\bar{p}$ while keeping the specimen, gas and temperature fixed. For each plateau, k_{app} is evaluated from the compressible Darcy law together with $\Delta(p^2) = p^2_u - p^2_d$. Introducing $x=1/\bar{p}$ and $y=k_{app}$ gives a linear relation:

$$y = k_\infty + (k_\infty b)\, x$$

3.5. Practical requirements and limitations of the method

The method is sensitive to several practical factors. Bear [44] emphasized the importance of pressure stability and the necessity of using precise regulators and throttling valves. Dullien [45] highlighted the significance of holder tightness and the elimination of bypass leakage. As noted in the literature, even temperature variations on the order of 0.1 °C can affect gas viscosity and measurement records; hence, isothermal conditions are recommended. Villar [22] confirmed the validity of using small specimens (e.g., Ø25 × 30 mm), provided that proper geometric scaling is applied.

3.6. Summary

In summary, the steady-state flow method with helium as the reference medium—as clearly demonstrated by Klinkenberg [43], Brace et al. [42], Bernabé [41], and Heap and Kennedy [40] represent the most reliable approach for assessing the permeability of concrete–coating systems with extremely low conductivity. Its application ensures high measurement sensitivity and comparability of results across laboratories. The use of helium not only facilitates the detection of extremely small flow rates but, when combined with the Klinkenberg correction, also provides permeability values that accurately reflect the intrinsic gas transport properties of the material, independent of pressure-dependent slip effects. Beyond methodological robustness, this technique offers critical interpretive value for engineering practice. By producing data that are representative of long-term performance under ACAES operating pressures, it allows for a realistic estimation of gas leakage rates and, consequently, storage efficiency. The method

therefore provides a direct link between laboratory-scale measurements and system-scale performance assessments, forming a necessary basis for the material qualification and coating selection required in shaft adaptation projects.

4. Laboratory setups

4.1. Introduction

The purpose of this section is to provide a detailed description of the laboratory apparatus shown in the photograph (*Figure 2*), designed to assess gas permeability in concrete–coating systems. While the fundamentals of the Steady-State Flow (SSF) method have already been presented in the *Methods* section, the focus here is on the construction and functionality of the experimental stand, its individual components, and the procedures used for sample preparation and operation. This ensures full technical documentation of the stand developed under WP4.

4.2. General concept

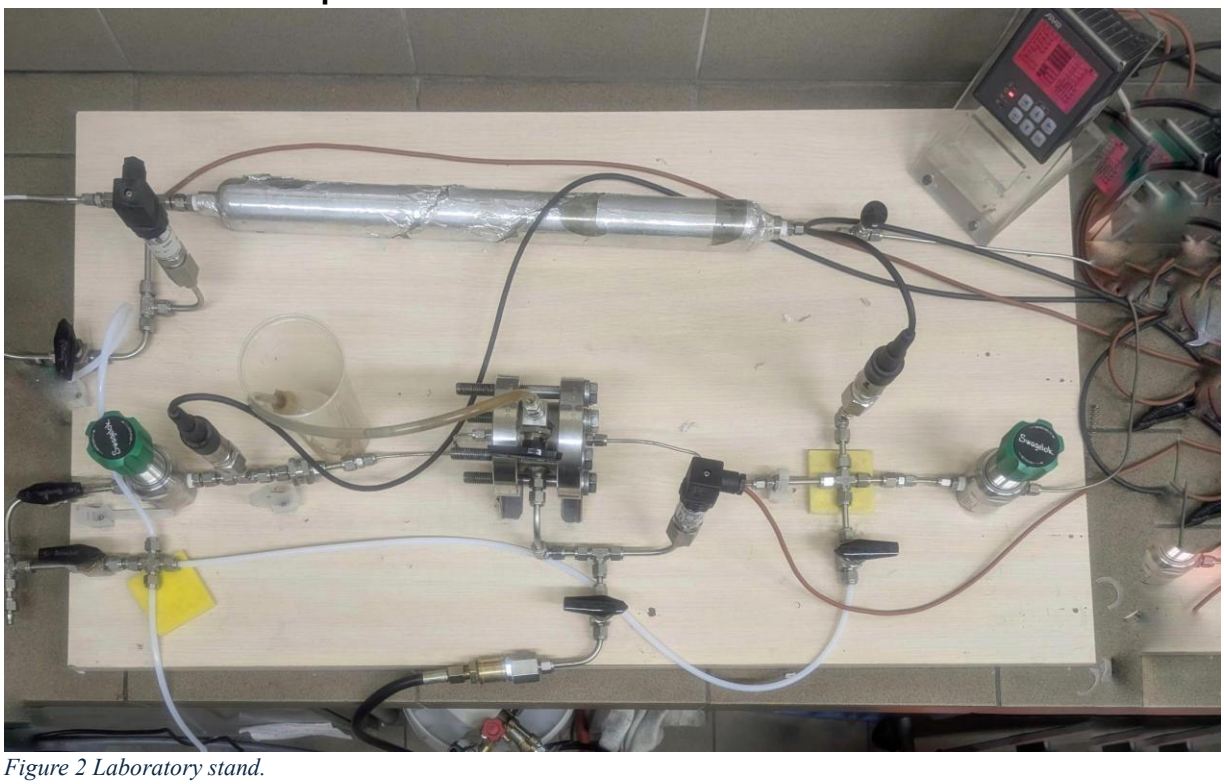

Figure 2 Laboratory stand.

The stand was designed for steady-state flow measurements on small cylindrical specimens (Ø25 × 30 mm) of concrete, both with and without protective coatings. The construction integrates precise pressure regulation, tight specimen sealing, and sensitive detection of very low flow rates. The operating pressure range 1-60 Bar and temperature stability around ±0,1 °C should be specified based on actual stand data. Similar approaches were described by Villar

[22] and Heap and Kennedy [40], who emphasize the importance of stable pressure regulation and isothermal conditions in studies of materials with very low permeability.

4.3. Setup architecture

The experimental stand is composed of a sequence of interconnected components ensuring precise regulation of inlet pressure, reliable sealing of the specimen, and accurate measurement of extremely low flow rates. The layout is illustrated in Figure 3, where the numbered elements correspond to the following functions:

1. Helium cylinder (99.999% purity) supplying the working gas.
2. Gas booster used to increase inlet pressure when required.
3. Compressor providing drive for the booster.
4. Inlet valve for switching and coarse regulation of the gas stream.
5. Pressure gauge and thermometer monitoring conditions directly after the inlet valve.
6. High-pressure reservoir (0.5 L, maximum 300 bar) stabilising supply pressure.
7. Secondary valve for isolating the reservoir from the specimen line.
8. Pressure gauge and thermometer installed downstream of the reservoir.
9. Specimen holder equipped with a silicone sleeve allowing application of confining pressure around 90 Bar ±2, preventing side leakage; fitted with pressure transducers upstream and downstream of the specimen.
10. Additional pressure gauge integrated in the holder for local verification of pressure conditions.
11. High-precision manometer ensuring accurate monitoring of the pressure drop across the specimen.
12. Flowmeter and data acquisition unit recording outlet gas flow and archiving signals from all sensors.
13. Hydraulic pump with water reservoir for generating and controlling confining pressure in the holder.

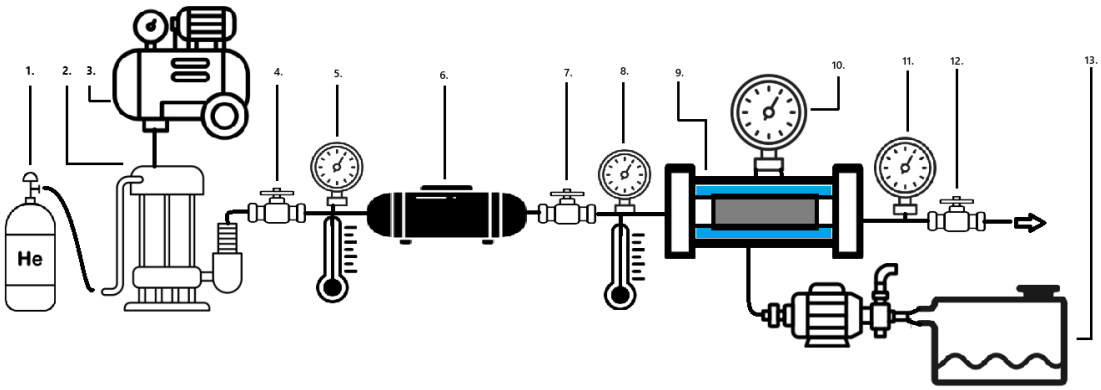

Figure 3 Lab stand.

This architecture ensures that the specimen is subjected to well-defined inlet and outlet pressures while side leakage is prevented by the confining system. Multiple pressure gauges and thermometers allow for cross-checking of measurement conditions, while the high-pressure reservoir and booster guarantee stable gas supply at the required operating pressures. The outlet side integrates a precision flowmeter and digital acquisition system, enabling detection of extremely low flow rates characteristic of coated concrete samples.

Table 3 Main technical parameters of the experimental setup.

Parameter	**Value/Specification**
Working gas	He
Operating pressure	60 to 50Bar or 60 to 1atm
Temperature control	Fixed at 20°C ±0,1 °C
Specimen dimensions	Ø25 mm × 30 mm
Concrete classes	C20/25 and C40/45
Coatings tested	WallCoat T, Sikagard M790
Confining pressure	90 Bar±2

4.4. Sample preparation and measurement procedure

Samples were made of concrete in accordance with EN 206 and EN 12390-2 [4–5]. Coatings were applied under controlled conditions in compliance with EN 1504-10 [9]. Specimens were cured for **90 days** to ensure compliance with EN 12390-2. The end faces were ground to achieve planarity and parallelism (per EN 12390-1 tolerances). Before testing, specimens were inspected for surface defects, and coating thickness was checked with a thickness gauge. Samples were then placed in a silicone sleeve (*Figure 4*), which, under confining pressure, ensured tightness.

Figure 4 Holder during installation of a coated concrete sample.

After installing the specimen, the system was flushed with helium to remove air. Inlet pressure was gradually increased using the regulator and needle valve, while lower, controlled pressure was maintained on the outlet side. Once inlet and outlet pressures, temperature, and flow reached a stable state, data acquisition began and continued until steady state was achieved. Measurements were carried out at various mean pressures.

4.5. Summary

The stand enables testing within operating pressures typical for ACAES but does not allow testing at elevated temperatures above or with aggressive technical gases other than helium and air. Another limitation is the small specimen diameter, which requires careful interpretation of results when scaled up to full-size structures.

The experimental stand combines precise pressure regulation, tight sealing of small specimens, and very sensitive flow detection, enabling permeability assessment of concrete–coating systems with extremely low conductivity. Its construction reflects both metrological rigor and the specific requirements of ACAES applications in mine shafts, providing a reliable platform for material evaluation within WP4. By combining standardized specimen preparation with advanced apparatus, the stand ensures repeatability and comparability of results across laboratories.

5. Results

5.1. Table of results

Table 4. Summary of gas permeability test results for concretes and coatings. The table includes the number of samples (n), mean permeability values, and sample standard deviations (SD). Data are presented separately for each material series and, where applicable, for both measurement ranges (60 to atm (atmospheric pressure) and 60 to 50 bar).

Table 4 Summary of gas permeability test results for concretes and coatings.

Material	Sample iD	60bar to atm [mD]	60 bar to 50 bar [mD]
C20/25	C20/25-1	5.02e-04	4.67e-04
	C20/25-2	4.33e-04	3.85e-04
	C20/25-3	4.89e-04	4.35e-04
	C20/25-4	5.02e-04	4.61e-04
	C20/25-5	4.33e-04	3.94e-04
	C20/25-6	4.89e-04	4.38e-04
Mean±SD		4.64e-04±3.20e-05	4.30e-04 ±3.39e-05
C40/45	C40/45-1	1.32e-04	-
	C40/45-2	1.45e-04	-
	C40/45-3	1.54e-04	-
	C40/45-4	1.25e-04	-
	C40/45-5	1.36e-04	-
	C40/45-6	1.32e-04	-
Material	Sample iD	60bar to atm [mD]	60bar to 50 bar [mD]
Sikagard ® M 790	C1-1	3.62e-08	3.11e-08
	C1-2	8.56e-07	7.69e-07
	C1-3	2.61e-08	2.32e-08
	C1-4	7.69e-07	6.88e-07
	C1-5	7.58e-07	6.74e-07
	C1-6	8.77e-07	7.83e-07
Mean±SD		5.54e-07 ± 4.08e-07	4.95e-07 ± 3.65e-07
WallCoat	C2-1	3.90e-08	-
	C2-2	3.20e-08	-
	C2-3	9.00e-09	-
	C2-4	5.10e-08	-
	C2-5	6.80e-08	-
	C2-6	2.10e-08	-
Mean±SD		3.67e-08 ± 2.11e-08	-

5.2. Permeability tests on concrete C20/25

Permeability measurements on concrete specimens of strength class C20/25 were conducted under two distinct pressure gradients: from 60 bar to atmospheric pressure and from 60 bar to 50 bar. This dual-gradient design was intentionally applied to provide a verification of the results and to test the robustness of the adopted methodology. The average permeability obtained under the 60 to atm configuration was 4.64×10^{-4} mD, while for the reduced 60bar to 50 bar gradient the mean result was 4.30×10^{-4} mD. In both cases, the variability of the data was modest, corresponding to only about 7% of the mean value, which is fully consistent with the expected experimental scatter for heterogeneous materials such as concrete.

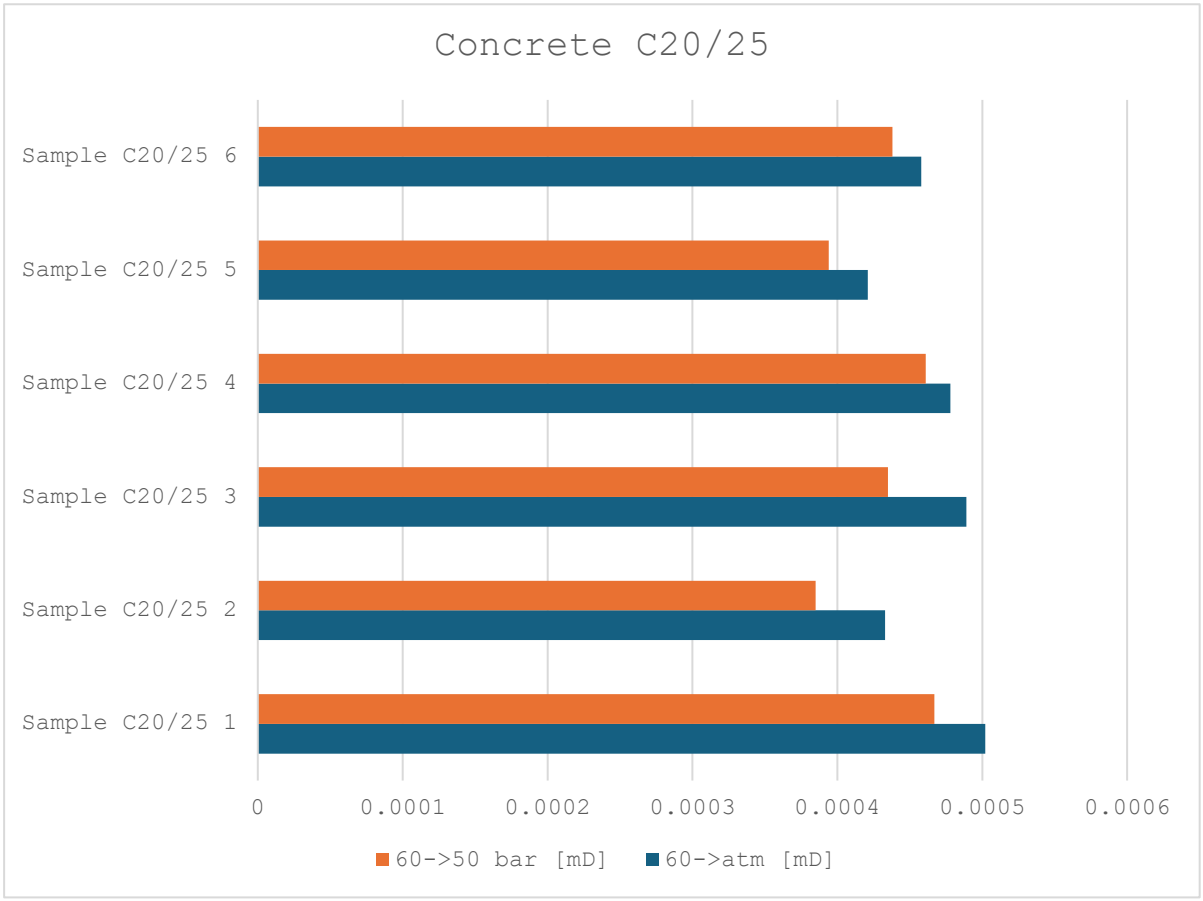

Figure 5 Permeability results for C20/25 concrete under two gradients: 60→atm and 60→50 bar

The comparison of these two independent test series shows that the permeability values remain within the same order of magnitude and differ by less than ten percent. This close agreement provides strong evidence for the reliability of the measurement procedure and confirms that the derived permeability coefficients are robust and not artefacts of the applied boundary conditions. The use of two pressure gradients therefore not only strengthened the confidence in the calculated values but also demonstrated the methodological soundness of the steady-state approach, laying the groundwork for meaningful comparisons with higher strength concretes and with coated specimens.

5.3. Permeability tests on concrete C40/45

The tests performed on concrete specimens of strength class C40/45 yielded average permeability values of 1.40×10^{-4} mD. The individual measurements ranged from 1.25×10^{-4} mD to 1.54×10^{-4} mD, and the variability of the results corresponded to approximately 7% of the mean. This level of scatter is typical for concretes, reflecting the heterogeneous pore structure, but it does not alter the overall interpretation of the dataset.

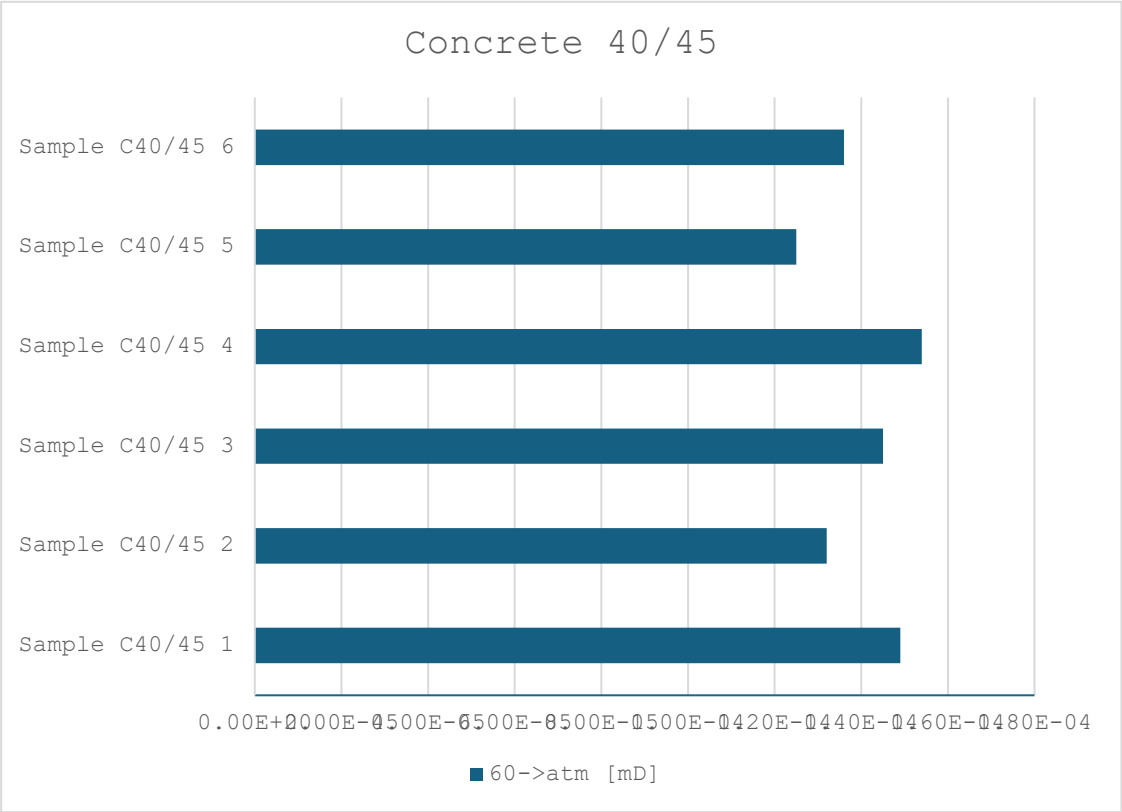

Figure 6Permeability results for C40/45 concrete.

In comparison with C20/25, the measured permeabilities for C40/45 were consistently lower by a factor of about three, confirming that the denser microstructure of higher strength concretes translates directly into a reduction of gas flow through the material. The close grouping of the data points and the moderate relative variability provide confidence that the observed difference is systematic rather than accidental. The results thus demonstrate that increasing concrete class is an effective measure to reduce leakage, although it does not fully eliminate measurable transport under elevated gradients.

5.4. Permeability tests on Sikagard® M 790

The application of the first coating system to concrete specimens resulted in a substantial reduction of permeability, with values reaching the order of 10^{-7} mD. For the 60→atm gradient, the average permeability was 5.54×10^{-7} , while under the reduced 60→50 bar gradient

the mean value was 4.95×10^{-7} mD. These values are several orders of magnitude lower than those recorded for uncoated concretes, confirming the high sealing efficiency of the applied barrier.

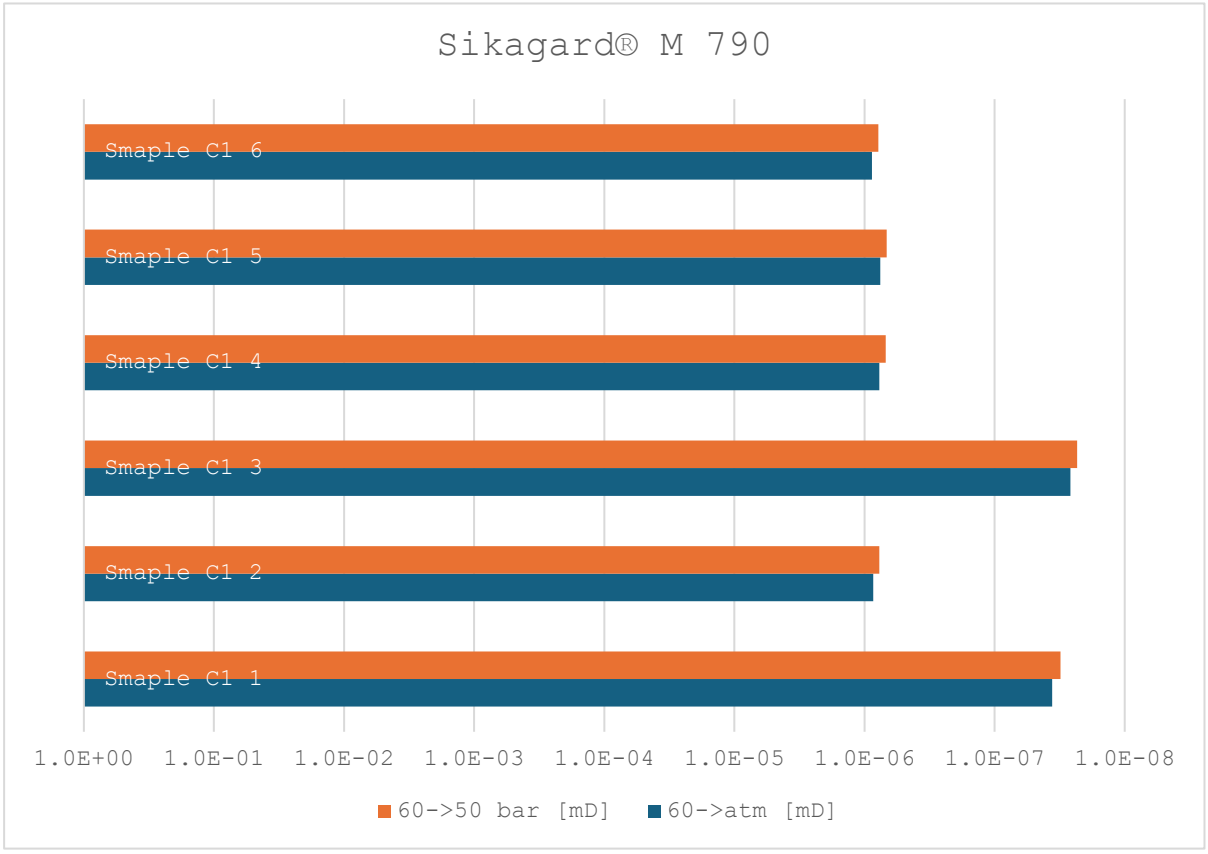

Figure 7 Permeability results for coating system under 60bar to atm and 60bar to 50 bar gradients.

However, the dataset also reveals a pronounced variability between individual samples. Standard deviations reached approximately 70–75% of the mean values, indicating that local heterogeneities within the thin coating layer had a strong influence on the measured transport properties. Such scatter is natural for thin-film systems, where factors such as micro-defects, local thickness fluctuations, and imperfect adhesion to the substrate can significantly affect permeability. Unlike bulk concrete, where the transport path averages across a thick matrix, coatings are sensitive to local weak spots which can dominate the overall gas flow. The comparison of both gradients (60 bar to atm and 60 bar to 50 bar) shows consistent mean results, confirming the validity of the computational approach and suggesting that the overall barrier performance of the coating is reliable despite local variability. The observed scatter therefore reflects the inherent microstructural sensitivity of thin layers rather than methodological errors. From a broader perspective, the results demonstrate that even with certain dispersion, coated systems deliver permeability values several orders of magnitude below those of uncoated concrete, which has direct implications for the long-term retention of pressurised gases.

5.5. Permeability tests on WallCoat T

The tests performed on coated specimens yielded an average permeability of approximately 5.0×10^{-8} mD. The individual measurements ranged from 2.1×10^{-8} to 9.0×10^{-8} mD, corresponding to a variability of nearly 50% relative to the mean. The pronounced scatter between samples is characteristic of thin-layer coating systems, where local heterogeneities such as micro-defects, irregular thickness, or application imperfections can significantly influence the measured permeability.

Despite the high variability, all results remain within the same order of magnitude, which confirms the correctness of the applied measurement procedure and indicates the stability of the results under the given pressure gradient.

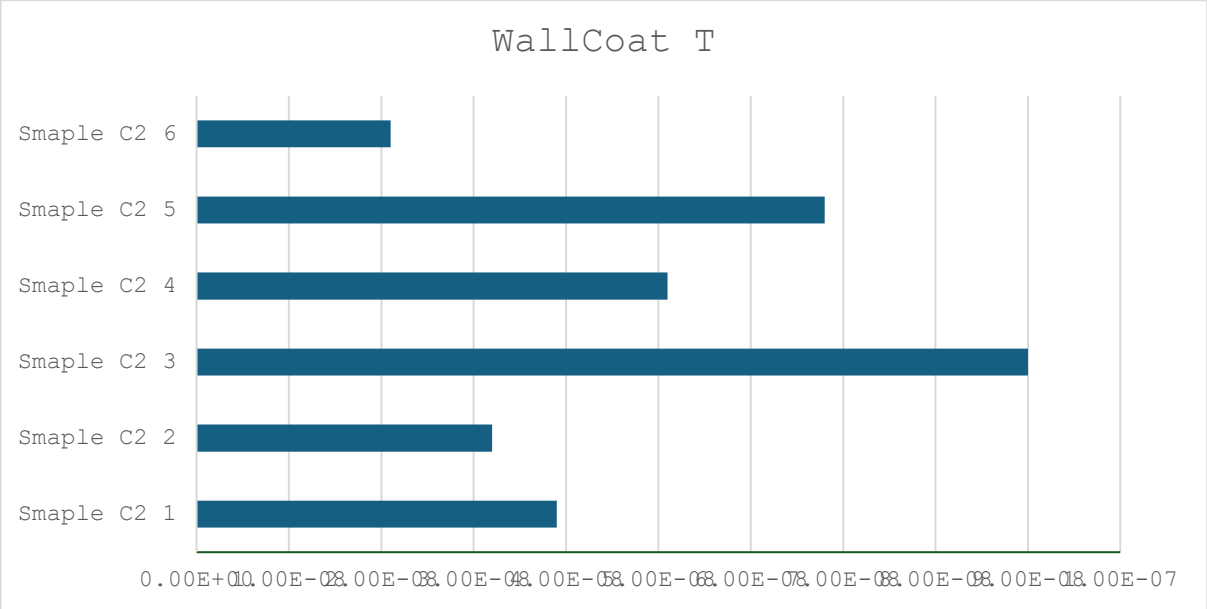

Figure 8 Permeability results for coating system under 60bar to atm.

5.6. Large-scale scenario: pressure losses in a cylindrical reservoir

In order to translate the laboratory-scale differences in permeability into an engineering context, a hypothetical storage reservoir was analysed in the form of a vertical cylinder with a diameter of 8 m and a height of 1000 m, filled with helium to an initial absolute pressure of 60 bar. The wall thickness was assumed to be 1 m, and gas migration was described under isothermal conditions using Darcy's law for compressible flow. Two material configurations were compared directly: uncoated concrete of strength class C20/25, and the same geometry lined internally with a polymer coating.

For the uncoated C20/25 concrete, characterised by an average permeability of 4.38×10^{-4} mD, the calculated pressure drop after 12 hours of leakage amounted to approximately 0.086 bar. In

contrast, for the coated system, with an average permeability of 7.69×10^{-7} mD, the corresponding loss was only about 0.00015 bar. This represents a reduction of nearly six hundred times in leakage rate due to the presence of the barrier coating.

The implications of this result are substantial. Differences in permeability observed at the specimen scale - on the order of three to four magnitudes - translate directly into dramatically different leakage dynamics when extrapolated to engineering-scale reservoirs. From the perspective of design and operation, such reductions in leakage not only increase the effective storage time but also enhance the safety and economic efficiency of the system. This analysis underscores the critical importance of surface protection technologies when considering the adaptation of concrete structures for high-pressure gas storage applications.

6. Applications

The results of the conducted research clearly confirm that the application of coating systems is an effective method of reducing gas permeability through concrete shaft linings adapted for compressed air energy storage. Measurements carried out on concretes of strength classes C20/25 and C40/45 demonstrated significant differences in permeability, reflecting the influence of microstructure and strength class on gas transport. Concrete C40/45 exhibited a permeability coefficient approximately three times lower than C20/25, which confirms that a denser microstructure results in reduced gas losses. Nevertheless, even higher-class concrete does not provide sufficient tightness in the context of the long-term storage of compressed gases.

The most important findings concern specimens coated with barrier systems. In both cases thin-layer epoxy systems and thick-layer Xolutec® membranes a reduction in permeability by three to four orders of magnitude compared to uncoated samples was achieved. This means that, under laboratory conditions, coatings effectively limit gas migration even under high pressure gradients (60 bar to atm), and their application is a necessary condition for adapting shafts for energy storage in the form of compressed air.

Differences between coating systems primarily concern variability of results and resistance to local defects. The epoxy coating, despite its high barrier efficiency, showed greater sensitivity to micro-defects and application-related irregularities, which translated into larger dispersion of measured values. The Xolutec® membrane, in contrast, due to its greater thickness and crack-bridging capacity, exhibited more stable performance under dynamic conditions and in environments prone to cracking. From an engineering perspective, this indicates different areas of application: thin epoxy layers may be used in shafts with high-quality concrete and limited deformation risk, whereas thick membranes are better suited for structures with elevated requirements and less favourable substrate stability.

Scenario calculations for a model cylindrical reservoir make it possible to translate laboratory findings into the engineering scale. The difference in pressure drop after 12 hours 0.086 bar for uncoated C20/25 concrete compared to only 0.00015 bar for a coated system proves that the use of barrier coatings may reduce gas losses by nearly six hundred times. This result has direct implications for the economic efficiency of ACAES systems, as limiting standby losses extends effective storage times and reduces operating costs.

In conclusion, the investigations carried out within Deliverable D4.3 unequivocally demonstrate the necessity of using protective coatings in the adaptation of mine shafts for compressed air storage. The obtained data provide reliable permeability coefficients for different material configurations, which can be directly applied in computational models and techno-economic analyses in subsequent stages of the HESS project. The document therefore forms a foundation for both design and strategic decisions, confirming the crucial role of materials engineering in transforming post-mining infrastructure into modern energy storage systems.

Literature

[1] EN 1504-2:2004. Products and systems for the protection and repair of concrete structures – Part 2: Surface protection systems for concrete. CEN, Brussels, 2004.

[2] EN 1504-10:2017. Products and systems for the protection and repair of concrete structures – Part 10: Site application of products and systems and quality control of the works. CEN, Brussels, 2017.

[3] Peng C., et al. Degradation Behavior and Lifetime Prediction of Polyurea Anti-Seepage Coating for Concrete Lining in Water Conveyance Tunnels. *Polymers*, 2024.

[4] EN 206:2013. Concrete – Specification, performance, production, and conformity. CEN, Brussels.

[5] EN 12390-2:2019. Testing hardened concrete – Part 2: Making and curing specimens for strength tests. CEN, Brussels, 2019.

[6] Olabi A.G., Wilberforce T., Ramadan M., Abdelkareem M.A., Alami A.H. Compressed air energy storage systems: Components and operating parameters – A review. Journal of Energy Storage, 2021, 34:102000.

[7] Bartela Ł., Ochmann J., Waniczek S., Rulik S., Lutyński M., Smolnik G. Evaluation of the energy potential of an adiabatic compressed air energy storage system based on a novel thermal energy storage system in a post mining shaft. Journal of Energy Storage, 2022, 54:105282.

[8] European Commission. The Just Transition Mechanism. Brussels, 2020.

[9] PN-G-05016:1997. Szyby górnicze — Obudowa — Obciążenia. Katowice, 1997.

[10] PN-G-05015:1997. Szyby górnicze — Obudowa — Zasady projektowania. Katowice, 1997.

[11] Wichur A. Zagadnienia projektowania obudowy szybów górniczych. Górnictwo i Geoinżynieria, 33(1), 2009, 407–436.

[12] RILEM TC 116-PCD. Preconditioning of concrete test specimens for the measurement of gas permeability and capillary absorption of water. Materials and Structures, 32 (1999), 174–176.

[14] EN ISO 7783:2018. Paints and varnishes – Determination of water-vapour transmission properties of coatings. ISO, Geneva, 2018.

[15] EN 1062-3:2008. Paints and varnishes – Coating materials and coating systems for exterior masonry and concrete – Part 3: Determination of liquid water permeability. CEN, Brussels, 2008.

[16] EN 1062-6:2002. Paints and varnishes – Coating materials and coating systems for exterior masonry and concrete – Part 6: Determination of carbon dioxide permeability. CEN, Brussels, 2002.

[17] STASICA J Nowoczesne metody badań i oceny stanu technicznego obudów szybów górniczych. Zeszyty Naukowe Instytutu Gospodarki Surowcami Mineralnymi i Energią Polskiej Akademii Nauk, nr 101, s. 85–100, 2017.

[18] European Commission. Communication from the Commission: The European Green Deal. COM(2019) 640 final. Brussels, 2019.

[19] ENTSO-E. TYNDP 2022 System Needs Study. Brussels, 2022.

[20] International Energy Agency (IEA). Energy Storage – Grid-scale storage (overview and data). Paris, 2024.

[21] European Patent Office. EP 3 792 467 B1 — Underground compressed air storage system. 2023.

[22] Villar M.V. Gas and Water Permeability of Concrete. Springer, 2012.

[23] ASTM D4060-19. Standard Test Method for Abrasion Resistance of Organic Coatings by the Taber Abraser. ASTM International, West Conshohocken, 2019.

[24] EN 1542:1999. Products and systems for the protection and repair of concrete structures – Test methods – Measurement of bond strength by pull-off. CEN, Brussels, 1999.

[25] Kim, D.S.; Kim, U.; Liyew, G.; Lee, C.-Y. Comparative analysis of air permeability between UHPC and epoxy-coated normal concrete. *Heliyon*, 2024, 10(23): e40598.

[26] Park, D.-C. Carbonation of concrete in relation to CO_2 permeability and degradation of coatings. *Construction and Building Materials*, 2008, 22(11), 2260–2268.

[27] Cabrera, C.; Ortega, L.; Fernández, J. Role of surface coatings in reducing CO_2 permeability of concrete structures. *Cement and Concrete Composites*, 2019, 104:103401.

[28] Li, M.; Xu, P.; Zhao, W. Comparative study on adhesion and permeability of epoxy and polyurethane coatings applied on concrete. *Journal of Materials in Civil Engineering*, 2018, 30(9): 04018200.

[29] EN ISO 7783:2018. Paints and varnishes – Determination of water-vapour transmission properties of coatings. ISO, Geneva, 2018.

[30] EN 1062-3:2008. Paints and varnishes – Coating materials and coating systems for exterior masonry and concrete – Part 3: Determination of liquid water permeability. CEN, Brussels, 2008.

[31] EN 1062-6:2002. Paints and varnishes – Coating materials and coating systems for exterior masonry and concrete – Part 6: Determination of carbon dioxide permeability. CEN, Brussels, 2002.

[32] EN 1062-7:2004+A1:2007. Paints and varnishes — Coating materials and coating systems for exterior masonry and concrete — Part 7: Determination of crack bridging properties. CEN, Brussels, 2007.

[33] Schiessl, P.; Breit, W. Crack-bridging behaviour of surface protection systems under dynamic loading. *Materials and Structures*, 2007, 40:79–92.

[34] Xu, T.; Zhang, J.; Li, H. Performance evaluation of crack-bridging protective coatings for concrete structures. *Construction and Building Materials*, 2020, 261:119948.

[35] EN 1542:1999. Products and systems for the protection and repair of concrete structures – Test methods – Measurement of bond strength by pull-off. CEN, Brussels, 1999.

[36] Sika Services AG. Product Data Sheet: Sikagard® M 790. Zürich, 2022.

[37] Cabrera, J.G.; Al-Khaja, W. Performance of epoxy and polyurethane coatings in marine environments. *Cement and Concrete Composites*, 1996, 18(6):409–419.

[38] Bicanic, N.; Mangat, P.S. Performance of crack-bridging surface protection systems for reinforced concrete structures. *Materials and Structures*, 1992, 25:445–452.

[39] Ye, H.; Jin, X.; Chen, Y. Comparative study on crack-bridging ability of epoxy and polymer-modified coatings. *Journal of Materials in Civil Engineering*, 2019, 31(12):04019373.

[40] Heap, M.J.; Kennedy, B.M. Exploring the scale-dependent permeability of fractured and intact volcanic rocks. *Journal of Volcanology and Geothermal Research*, 2016, 327:520–530.

[41] Bernabé, Y. The effective pressure law for permeability in Chelmsford granite and Barre granite. *International Journal of Rock Mechanics and Mining Sciences & Geomechanics Abstracts*, 1989, 26(5):535–546.

[42] Brace, W.F.; Walsh, J.B.; Frangos, W.T. Permeability of granite under high pressure. *Journal of Geophysical Research*, 1968, 73(6):2225–2236.

[43] Klinkenberg, L.J. The permeability of porous media to liquids and gases. *API Drilling and Production Practice*, 1941:200–213.

[44] Bear, J. *Dynamics of Fluids in Porous Media*. Academic Press, New York, 1972.

[45] Dullien, F.A.L. *Porous Media: Fluid Transport and Pore Structure*. Academic Press, San Diego, 1992.

[46] Liu, Y.; Yang, Z.; Chen, F. Performance of protective coatings for concrete structures under pressurized air permeability tests. *Materials and Structures*, 2021, 54:27.